

Neutron Dosimetry and Monitoring in the Radiation Environment

Takashi Nakamura

*Cyclotron and Radioisotope Center, Tohoku University
Aoba, Aramaki, Sendai 980, Japan*

1. INTRODUCTION

A rapid increase of nuclear facilities for their widespread application makes important the neutron dosimetry and monitoring in the surrounding environment. Neutron leakage and its long-distance propagation in the atmosphere from intense neutron facilities and high energy accelerator facilities are especially important for the shielding design of facilities and the resulting dose reduction to nearby population, because of the strong penetrability of high energy neutrons.

The measurement of neutron energy spectrum and dose equivalent in the environment requires the following technological problems.

1) Neutrons always accompany with gamma rays, which requires the gamma-ray insensitive detector or the neutron-gamma-ray discrimination technique.

2) The neutron energy distributes in a wide energy range from thermal to high energy, and no single detector is possible to give this wide energy spectrum.

3) The neutron quality factor is strongly dependent on the neutron energy.

The neutron dose equivalent, H can be obtained in the following three ways;

In the radiation environment around nuclear

i) by using various spectrometers,

$$H = \int K(E)\phi(E)dE,$$

where

K(E) = conversion factor,
 $\mu\text{Sv per n/cm}^2$,

$\phi(E)$ = energy spectrum, $\text{n}/(\text{cm}^2 \cdot \text{MeV})$

ii) by using LET spectrometer,

$$H = \int Q(L)D(L)dL,$$

where L = linear energy transfer,
LET, $\text{keV}/\mu\text{m}$

Q(L) = quality factor,

D(L) = LET spectrum, Gy per LET

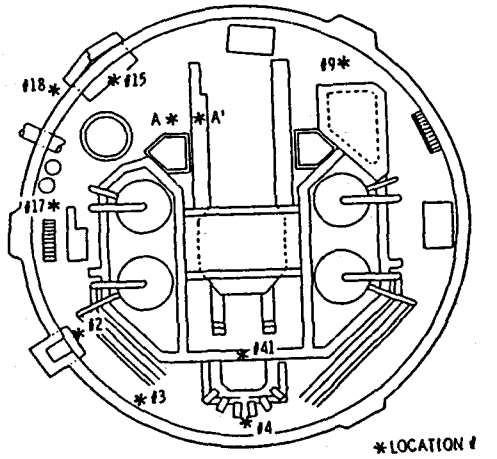
iii) by using dose equivalent counter,

where

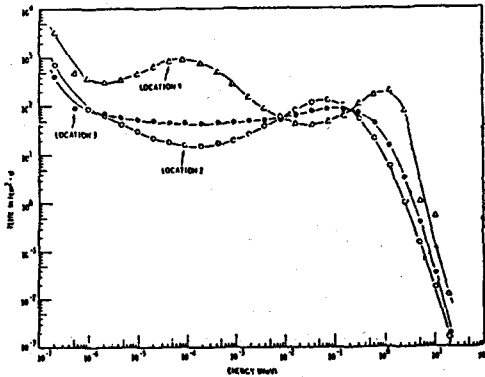
K = calibration constant,
 $\mu\text{Sv per counts}$,

P = counts.

facilities, neutrons have energies extended from thermal to several tens of MeV. One example[1] is the neutron spectrum measurement in the PWR facility shown in Fig. 1. On the operating deck above the reactor core, the measured spectra at some locations have a dominant fraction in the intermediate energy region between thermal and MeV, and close to a 1/E slowing-down spectrum. Another example[2] is the neutron spectrum in the 1 GeV electron synchrotron facility shown in Fig. 2.



Site G, Operating Deck Measurement Locations



Site G, Neutron Flux Versus Energy Measured by Multisphere Spectrometer

Fig.1. Neutron spectra on the operating deck above the reactor core of PWR [1].

The source neutrons produced via photoneuclear reaction from the synchrotron ring have fission-like spectrum in the low energy region and also have high energy tails. In contrast to the source spectrum, neutrons penetrated through a 75-cm thick concrete shield have a 1/E slowing-down spectrum in the intermediate energy region.

2. DETECTORS FOR ENVIRONMENTAL NEUTRON MEASUREMENT

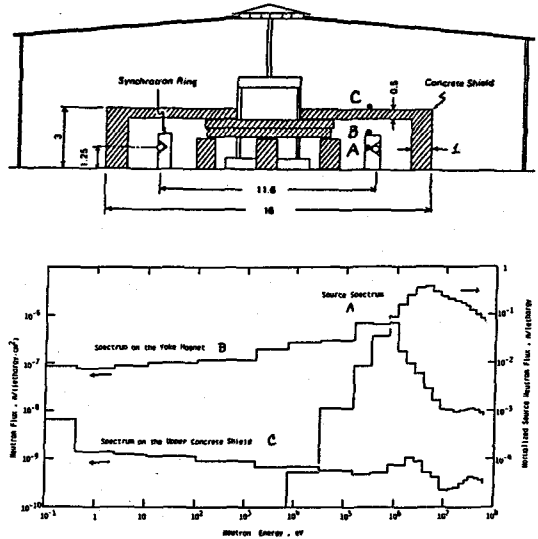


Fig.2. Neutron spectra around the source produced by photonuclear reaction in the 1 GeV electron synchrotron facility [2].

There are many neutron spectrometers and dosimeters usable in area monitoring and personal monitoring. Figure 3 shows their applicable energy range. In the thermal energy region and above about 100 keV, several detectors can be used for spectroscopy, while in the wide energy range from 1 eV to 100 keV, the multi-moderator spectrometer is the only one detector for spectroscopy, except the TOF method. The rem counter is widely used for environmental neutron dosimetry.

As for personal monitoring, albedo dosimeter was the only one method to measure the dose of intermediate energy neutrons, but now the superheated drop detector begins to be used as an active dosimeter[3]. We are now developing a real time wide energy range dosimeter using two types of silicon detectors[4].

For the environmental neutron measurement, the multi-moderator spectrometer, so-called

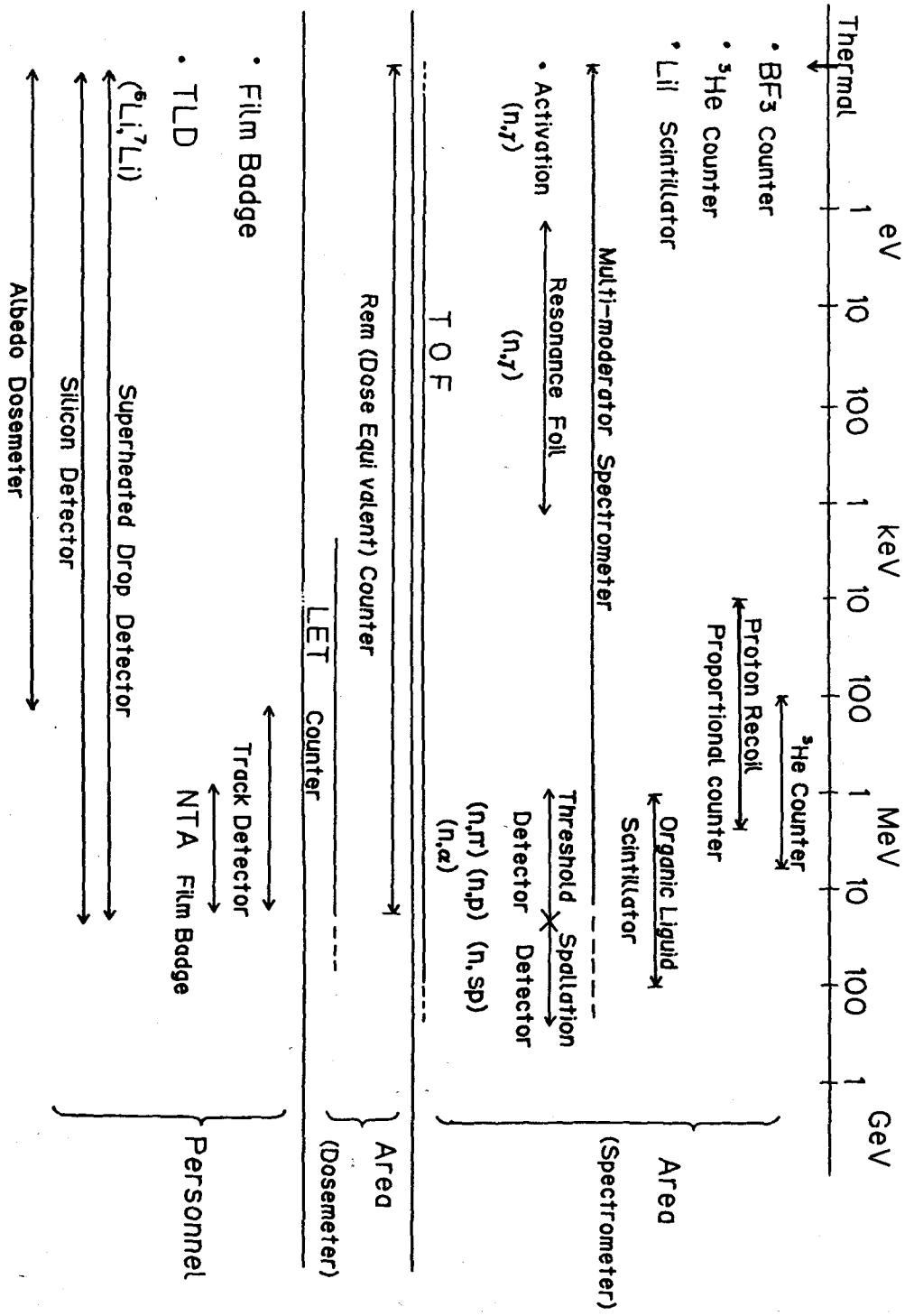


Fig. 3. Neutron spectrometers and dosimeters and their applicable energy range

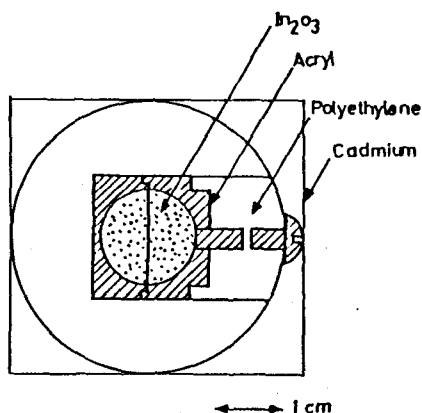


Fig. 4. Cross sectional view of the indium activation multi-moderator neutron spectrometer. The hatched and dotted parts are the activation detector. The radii of the spherical moderators are 983, 533, 322 and 203 cm [5].

Bonner ball, is a unique easy-handling detector which gives the whole energy spectrum from thermal through MeV. We have developed two types of Bonner ball [5]. One is a gamma-ray insensitive type, which can be used in the gamma-ray dominant pulsed neutron field. An indium activation detector is loaded in the center of the polyethylene moderator of various thicknesses. A cross-sectional view of the 203-cm radius detector is shown in Fig. 4. The hatched central part of cylindrical acryl has a dotted spherical hole of 0.735 cm radius which is filled with indium oxide. The other is a high efficiency type which contains a 51-cm diam. 10-atm ^3He proportional counter in the center of the polyethylene sphere. This spectrometer is useful for low level neutron measurement. All moderators are covered with a 1-mm thick cadmium cover to cut off thermal neutrons.

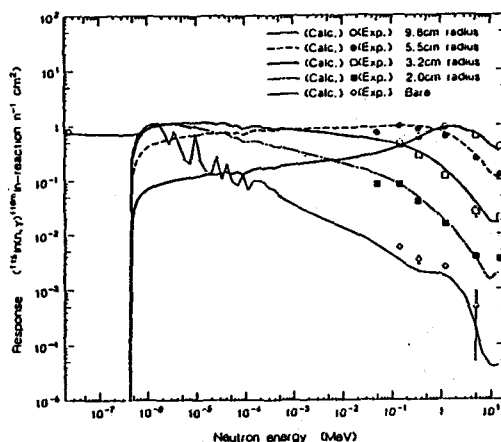


Fig. 5. Measured and calculated response functions of the indium activation multimoderator spectrometer [5].

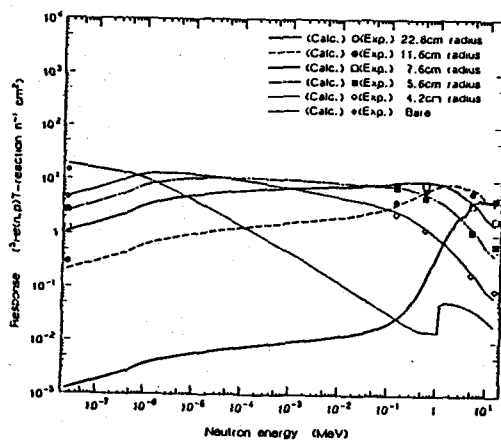


Fig. 6. Measured and calculated response functions of the multi-sphere moderated ^3He counter [5].

The response functions of these two spectrometers were calculated by the one-dimensional discrete ordinate transport code, ANISN. The calculational accuracy was checked by using thermal and monoenergetic neutron standard fields at the Electro-Technical Laboratory. Figures 5 and 6 show the calculated response functions together with

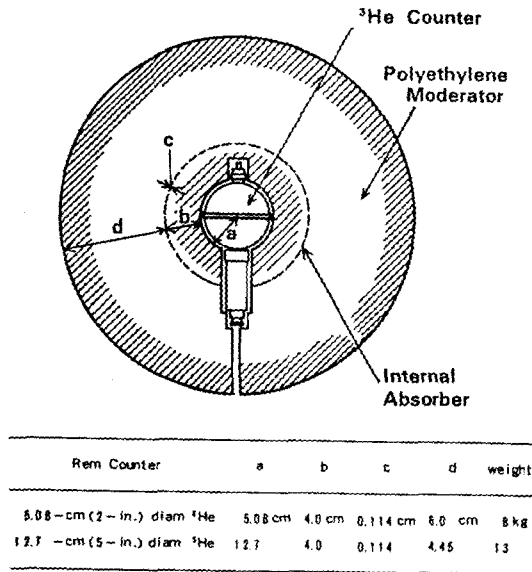


Fig. 7. Cross-sectional view of our high sensitivity rem counters and their sizes with a 508-cm-diam and a 127-cm-diam ^3He counter [6].

measured results[5].

The measured and calculated responses show generally good agreement. The gross feature of neutron spectrum can be obtained by unfolding the counting rates using the differing energy responses as a function of moderator thickness.

We have also realized two types of high sensitivity rem counters by using large volume and high pressure ^3He counters[6]. One is filled with 10 atm ^3He having 51 cm diameter and the other is filled with 5 atm ^3He having 127 cm diameter. Figure 7 shows the cross-sectional view of our rem counters.

The responses to neutron energy from thermal to 15 MeV were experimentally determined by using the same standard field as above. Figure 8 shows the measured data compared with the flux-to-dose equivalent conversion factor defined by the ICRP-21[7]. Our two rem counters, which are called as 2-in(51 cm)

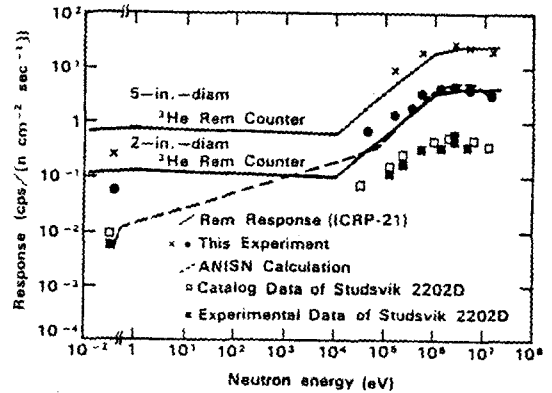


Fig. 8. Measured neutron energy responses of our 2-in-diam and 5-in-diam ^3He and Studsvik 2202 D rem counters. The ICRP-21 ideal rem response and the calculated detector responses by the ANISN code are also shown for comparison [6].

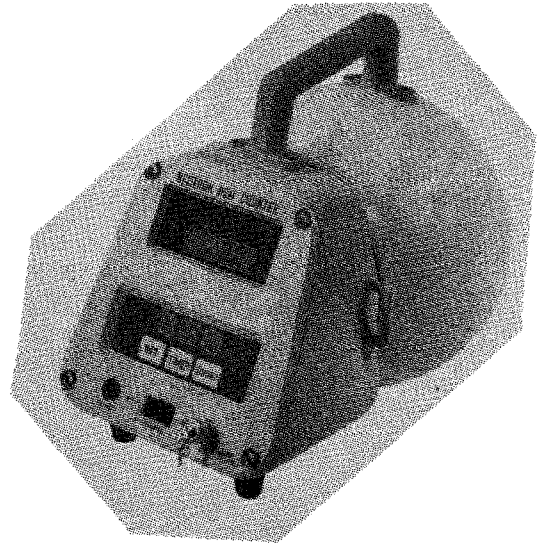


Fig. 9. External appearance of commercial high efficiency dose equivalent counter by Fuji Electric Co., Ltd.

diam ^3He rem and 5-in(127 cm) diam ^3He rem, have good characteristics in that the responses are well fitted to the ICRP-21 rem response.

The 2-in diam and 5-in diam ^3He rem counters have about 10 times and 70 times higher sensitivities, respectively, than the widely-used Studsvik 2202 D rem counter. Our rem counters have spherical shapes to avoid the directional dependence of their sensitivities for omnidirectional injection of environmental neutrons. The 2-in diam ^3He rem counter in Fig. 9 is now commercially available from Fuji Electric Co Ltd.

3. ENVIRONMENTAL NEUTRON MEASUREMENT

By using these detectors, we performed neutron measurement in the environment surrounding various nuclear facilities and also in the aircraft flying over Japan. I will exemplify two experiments.

(1) Skyshine from a 14 MeV d-T Neutron Source Facility[8].

A long-distance neutron propagation in the air-over-ground mainly due to the skyshine effect was measured around the intense 14 MeV d-T neutron source facility of Department of Nuclear Engineering at Osaka University.

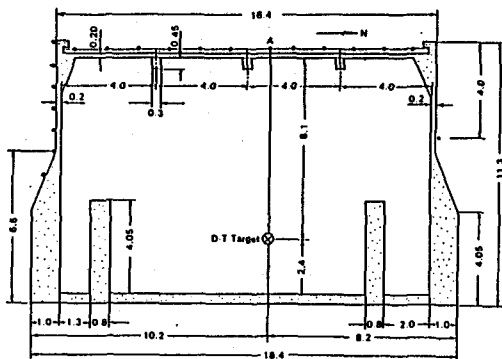


Fig.10. Source geometry of the skyshine experiment at the OKTAVIAN 14-MeV neutron source facility. Measurements are in metres.

Figure 10 shows the source geometry of the experiment. The 14-MeV neutrons were generated from the d-T reaction at the DT target as indicated by in the figure. The concrete wall thickness is 20 cm on the roof, 20 cm at the upper part of the side wall, and 1 m at its lower part. The building is 105 m high and a rectangle 164 m long from north to south and 315 m long from east to west. The neutron energy spectrum was measured by the Ne-213 scintillator and the ^3He -loaded Bonner ball only at Position A, just above the target. Figure 11 shows the neutron energy spectrum at Point A. The left spectrum was given by the NE-213 scintillator and the right spectrum by the Bonner ball. The measured spectra are compared with the discrete ordinate calculation by the ANISN and DOT 35 codes. There can be seen neutron components lower than 14 MeV due to scattering with concrete. Except for large oscillative errors in the energy region just below a sharp prominent 14 MeV peak of the measured data coming from unfolding, the agreement between experiment and calculation is satisfactory in absolute value.

Figure 12 shows the detecting points in the environment drawn as black circles and labeled with their distances from the tritium target, as well as the topology and arrangement of the buildings. The neutron spectra and doses were measured with the NE-213 scintillator, ^3He loaded Bonner ball and high-efficiency rem counter. The detecting points extend up to about 600 m far from the target. Figure 13 shows the skyshine neutron spectra at 99 m away from the target. The spectrum measured with Bonner ball is compared with discrete ordinate and Monte Carlo calculations. The measured spectrum gives good agreement with those calculations. But the MMCR-2 Monte Carlo results do not include the directly-coming

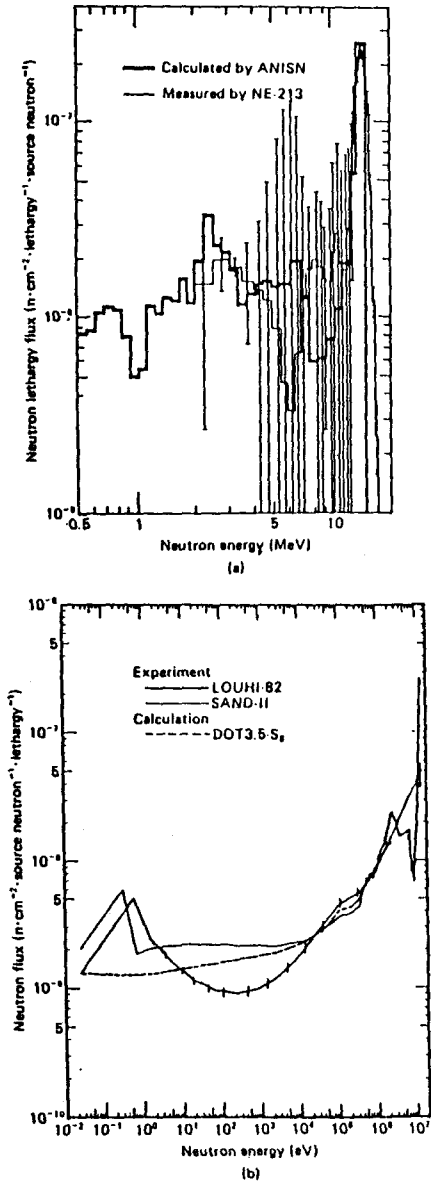


Fig. 11. Comparison of measured and calculated neutron spectra on the roof just above the target, point A in Fig 10 : (a) the spectrum in the mega-electron-volt region measured by the NE-213 detector compared with the ANISN calculation and (b) the whole spectra unfolded by the LOUHI-82 and SAND-II codes from the data measured with the ³He Bonner ball compared with the DOT 3.5-S₈ calculation[8].

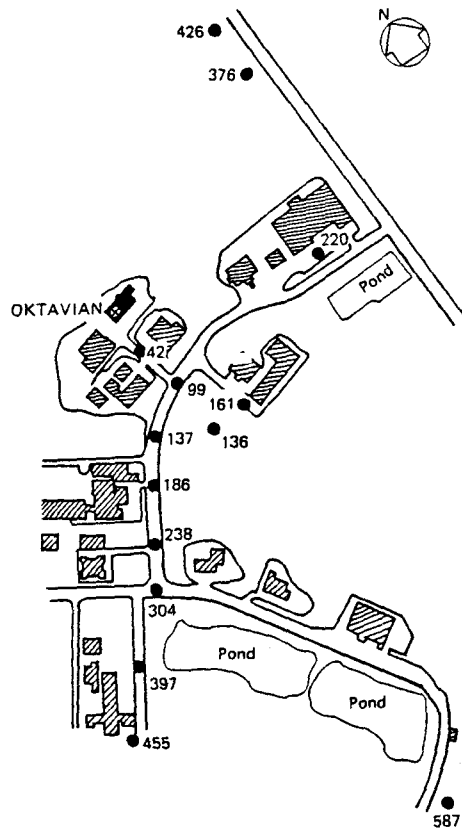


Fig. 12. Detection points(black circles)around the OKTAVIAN building for the skyshine experiment. The distances from the tritium target are given in metres.

neutrons from the target without collision and then give a little lower values than the other results below about 1 keV and near 14 MeV. In this skyshine spectrum, the 1/E slowing-down component is clearly seen in the energy range below 100 keV, in addition to the remaining 14 MeV source neutrons.

Figure 14 shows the environmental neutron dose distributions measured with the Studsvik 2202 D rem counter and our high efficiency 5-in

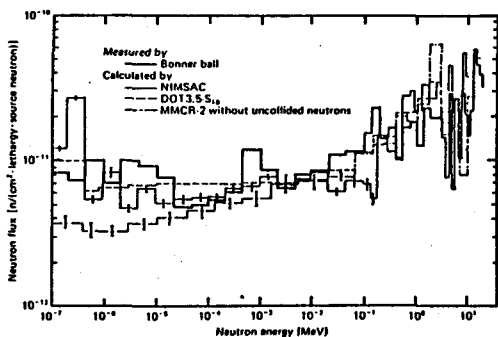


Fig. 13. Comparison of measured and calculated neutron spectra in the field at 99 m from the source (8)

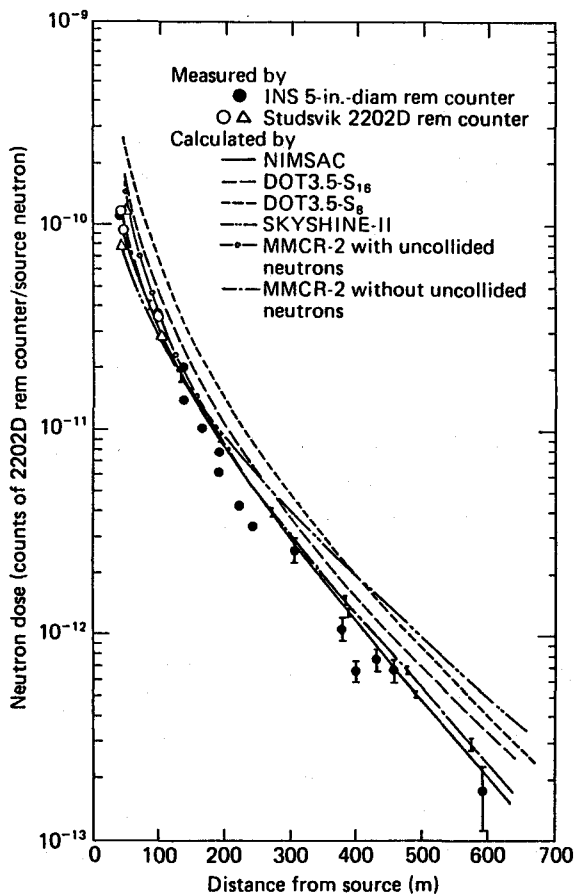


Fig. 14. Comparison of measured and calculated neutron dose distributions in the field around the OKTAVIAN building.

diam ³He rem counter. By using our rem counter, we could measure very low level neutron dose, about 004 μ rem/h at 600 m away from the target in only a few hours counting time. This dose level is only about one-tenth of the background neutron level coming from cosmic-ray neutrons. The measured data are compared with various calculations. The Monte Carlo results by NIMSAC and MMCR-2 give very good agreement with the measured results within about 30%, except some data. The DOT 3.5-S₇ results give values about twice as large as the measured results, but the DOT 3.5-S₁₆ results become much closer to the experiment. The SKYSHINE-II results indicate gradual overestimation with increasing distance. At some points, the measured data are lower than the Monte Carlo results. This discrepancy can be explained by the shielding effect of the nearby tall buildings and hill.

(2) Analytical Representation of Skyshine Effect

This skyshine effect of neutrons and also secondary gamma rays was analyzed by the Monte Carlo code MMCR-2 developed by us[9]. The calculated dose distributions of neutrons D_n and secondary gamma rays D_r are well fitted to the following analytical formula.[9, 10]

$$D_n(r) = \sum_i \sum_j \frac{Q_n(E_i, \theta_j)}{r} e^{-r/\lambda_n(E_i, \theta_j)} S(E_i, \theta_j) \Delta E_i \Delta \Omega_j$$

$$D_r(r) = \sum_i \sum_j \frac{Q_r(E_i, \theta_j)}{r} e^{-r/\lambda_r(E_i, \theta_j)} S(E_i, \theta_j) \Delta E_i \Delta \Omega_j$$

where $S(E_i, \theta_i)$ = source neutron intensity

of energy E_i at angle θ_i ,
 λ and $Q =$ fitting parameters,

$r =$ slant distance from source to detector.

This skyshine analysis was performed by Alsmiller et al. by using the DOT 3.5 code[11]. Stevenson and Thomas[12]also introduced a very simple analytical formula from Alsmiller results, as follows,

$$D_n(r) = Q_n(E_0) e^{-\lambda/\lambda_n(E_0)/r^2}$$

where $E_0 =$ incident particle energy.

This formula assumes the $1/E$ neutron spectrum up to incident particle energy and then is possible to apply mainly for high energy accelerator facilities.

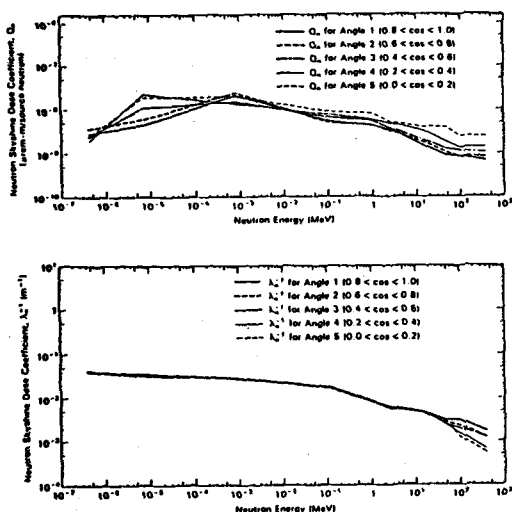


Fig.15. Dependence of Q_n and λ^{-1}_n on the source neutron energy E_s and angle θ_s for a neutron source fixed 15 m above the ground [10].

The parameters of Q_n and λ_n of our formula are shown in Fig. 15 when the neutron source situates 15 m above the ground. By using these parameters, we can easily calculate the

skyshine neutron and secondary gammaray doses only knowing the source neutron spectrum S . Our analytical formula was applied to estimate the skyshine neutron dose distribution around this 14 MeV d-T neutron source facility. The formula well fits the measured results and gives a little safer values, as shown in Fig. 16.

(3) Cosmic-Ray Neutron Measurement[12].

The next experiment is the measurement on the altitude variation of cosmic-ray neutron energy spectrum and dose equivalent. The data were obtained from a 2 hour flight of a DC-8

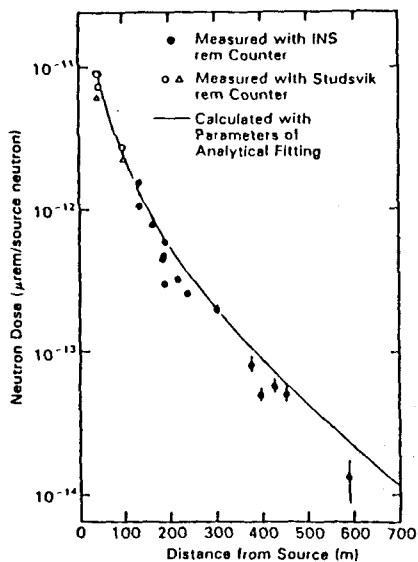


Fig. 16. Comparison of measured and calculated neutron dose distributions as a function of distance from the source in the OKTAVIAN skyshine experiment [10].

aircraft of Japan Air Lines chartered by the Institute for Physical and Chemical Research. The previous measurements are mostly limited to geomagnetic latitudes beyond about 40°N. In our study, the altitude variation of cosmic ray neutrons was measured at 24°N latitude in the

atmosphere over Japan. High efficiency multi-moderator spectrometer and rem counter described were set in the aircraft. The flight started from Narita airport proceeded west, keeping the geomagnetic latitude at 24°N and returned to Narita. During 2 hour flight, the aircraft was cruising for 60 min at an altitude of 4,880 m and for 20 min at 11,280 m for spectral measurements. The flight path is plotted in Fig. 17.

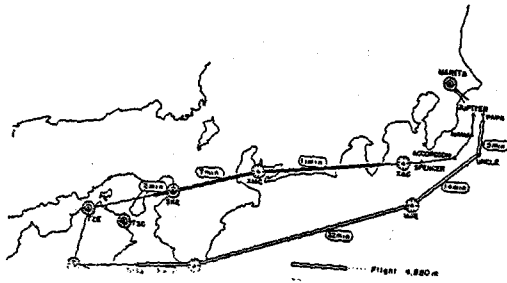


Fig. 17. Path of the DC-8 flight chartered by IPCR (Institute for Physical and chemical Research) on Feb 27, 1985.

Figure 18 shows the altitude variation of neutron dose equivalent rates measured by the high efficiency rem counter. The measurements were carried out in 1 or 2 min counting times. Dose equivalent rates were also obtained from the Bonner ball at 4,880 m and 11,280 m above sea level. The dose equivalent rates given by the Bonner ball agree very well with those by the rem counter. The dose equivalent rates increase according to a quadratic curve up to about 6,000 m and linearly beyond 6,000 m. At 10,000 m the dose equivalent rate is about 100 times higher than at sea level.

Neutron energy spectra were measured with the Bonner ball at 4,800 m, 11,280 m and at sea level. Figure 19 shows the unfolded energy spectra in lethargy unit from thermal to 400

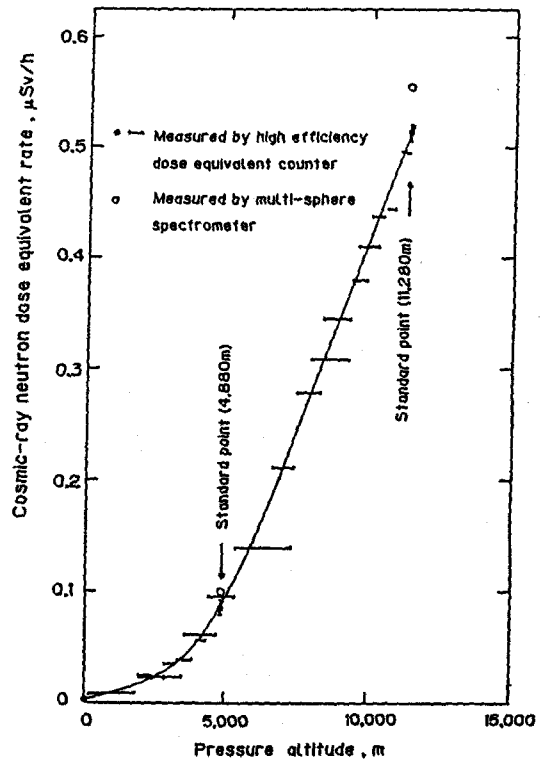


Fig. 18. Altitude variation of neutron dose equivalent rates measured by the high efficiency neutron dose equivalent counter [13].

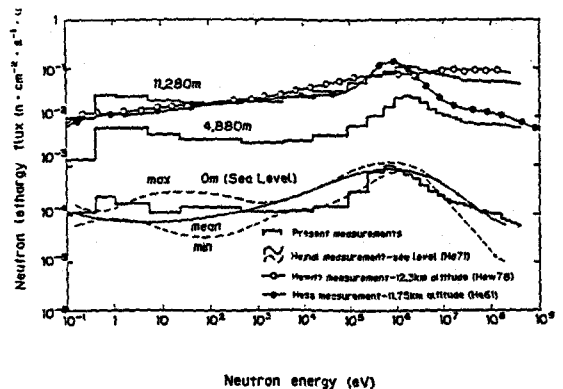


Fig. 19. Comparison of measured neutron lethargy spectra with other experimental spectra by Hess, Hajnal and Hewitt [13].

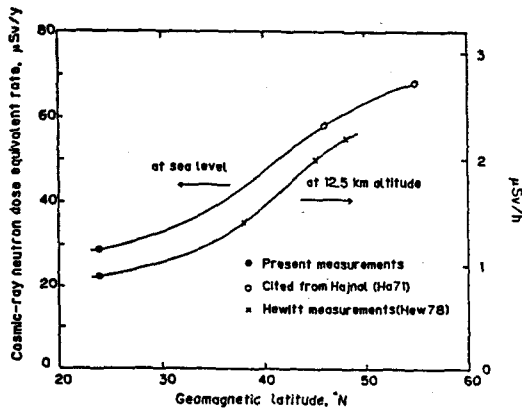


Fig. 20. Variations of neutron dose equivalent rate with geomagnetic latitude in north hemisphere [13].

MeV. At sea level, our spectrum at 24°N is compared with that of Hajnal et al. at 41°N [14]. The agreement is quite good in general despite the differences in the geomagnetic latitudes. At 11,280 m, our spectrum at 24°N [15] and that of Hewitt et al. measured at 12,300 m at 507°N [16]. In the energy region below 100 keV, these three spectra are close to 1/E slowing down spectrum. Our spectrum has an evaporation peak similar to that of the Hess spectrum and is in agreement with the Hewitt spectrum beyond the evaporation peak. With decreasing altitude, that means, increasing air depth, the high energy neutrons become less and the spectrum becomes softer due to multiple collision with air.

Figure 20 shows the dose equivalent rates at sea level and at 12,500 m altitude plotted as a function of geomagnetic latitude. Except for the data for 41°N at sea level, all data lie on two smooth curves that increase with geomagnetic latitude. This result reflects the fact that the production of secondary cosmic ray neutrons in the atmosphere is decreased at lower latitudes, due to the wellknown geom-

agnetic effect that incoming primary protons of low energy are screened out by the Earth's magnetic field at lower latitudes.

SUMMARY

The high efficiency moderated-type neutron spectrometer and dose equivalent counter were developed for the measurement of low level environmental neutrons. By using these detectors, the neutron energy spectra and dose equivalent rates due to skyshine effect were measured in the environment surrounding the accelerator facilities and also the altitude variation of cosmic ray neutrons in the aircraft flying over Japan.

REFERENCES

1. G.W.R. Endres et al, NUREG/CR-1769, PNL-3585, Pacific Northwest Laboratory (1981).
2. T. Nakamura and K. Hayashi, *Proc. 6th Intern. Conf. on Radiation Shielding*, Vol. II, p 1017, May 16-20, Tokyo (1983).
3. R.E. Apfel and S.C. Roy, *Radiat. Prot. Dosim.*, 10, 327 (1985).
4. T. Nakamura, M. Horiguchi, T. Suzuki and T. Yamano, *Radiat. Prot. Dosim.*, 27, 194 (1989).
5. Y. Uwamino, T. Nakamura and A. Hara, *Nuc 1 Instrum Methods*, A 239, 299 (1985).
6. T. Nakamura, A. Hara and T. Suzuki, *Nuc 1. Instrum. Methods*, A 241, 554 (1985).

7. ICRP Pub 1 21, Int. Commission on Radiological Protection (1971).
8. T. Nakamura et al, *Nuc l. Sci. Eng*, **90**, 281(1985).
9. T. Nakamura and T. Kosako, *Nuc l. Sci. Eng*, **77**, 168(1981).
10. K. Hayashi and T. Nakamura, *Nucl. Sci Eng*, **91**, 332(1985).
11. RG. Alsmiller Jr, ORNL/TM-7512, Oak Ridge National Laboratory (1980).
12. GR. Stevenson and RH. Thomas, *Health Phys*, **46**, 115(1984).
13. T. Nakamura, Y. Uwamino, T. Ohkubo and A. Hara, *Health. phys*, **53**, 509(1987).
14. F. Hajnal, JE. McLaughlin, MS. Weinstein and K. O'Brien, USAEC Report HASL-241 (1971).
15. W.N. Hess, E.H. Canfield and RE. Lingenfelter, *JGeophys. Res*, **6**, 665(1961)
16. JE. Hewitt et al, *Health Phys*, **34**, 375(1978).